IUST
Iran University of Science and Technology

Iranian Journal of Electrical and Electronic Engineering

Journal Homepage: ijeee.iust.ac.ir

An Improved Procedure for Analysis of Distribution Networks Under Direct and Indirect Lightning Discharges

Peyman Gholami *, Nabiollah Ramezani * (C.A.) and Faridoddin Safaei*

Abstract: This study investigates overvoltages transmitted through low-voltage (LV) networks, which pose a significant risk to sensitive electronic devices. High-frequency component models of the LV network are employed to analyze overvoltages propagating through LV distribution transformers. To efficiently assess these transients, the Monte Carlo method is applied, enabling a focused analysis within a constrained simulation domain while reducing computational time. Furthermore, a protective algorithm is proposed to safeguard LV networks and connected loads against lightning-induced overvoltages. The study also evaluates the influence of significant mitigation measures, including spark-gap-based protection and the installation of surge protective devices (SPDs), on overvoltage suppression in LV distribution systems. Finally, the effects of lightning strikes on the load-side lightning protection system (LPS) and the resulting induced overvoltages in the LV network are investigated. The proposed network and its components are simulated using both MATLAB and ATP-EMTP to ensure comprehensive analysis. In addition to the computational efficiency achieved through the enhanced Monte Carlo method, the proposed methodology offers a practical and effective approach for improving overvoltage protection in LV distribution networks.

Keywords: Distribution network, transformer modelling, lightning overvoltages, Monte Carlo method.

1 Introduction

GIVEN the low height of overhead lines and the presence of nearby buildings and trees, direct lightning strikes on the lines are statistically improbable. Consequently, most strikes terminate on the adjacent ground surface in the vicinity of the lines [1]. Lightning strikes to nearby ground induce significant overvoltages on distribution lines through electromagnetic coupling, a well-documented phenomenon in power systems. These induced overvoltages can propagate through LV transformers, potentially causing severe damage to both distribution network equipment and connected low-voltage loads [2]. To address this challenge, it is necessary to evaluate the impact of high-frequency models on the distribution network and subsequently propose an appropriate set of protective measures. Consequently, numerous recent studies [1–7] have focused on assessing lightning-induced overvoltages in distribution networks. A common approach to reducing computational effort in calculating lightning-induced overvoltages involves the use of simplified formulas, such as Rusk's formula, as demonstrated in [8, 9]. In [10], the lightning performance of distribution lines was further investigated through analytical evaluation. Analytical methods rely on equations that require numerical integration, which can sometimes result in limited solution accuracy. Given the stochastic nature of lightning-induced overvoltages, the Monte Carlo method, a statistical approach offering acceptable accuracy, is commonly employed for overvoltage computation. The calculation of lightning-induced overvoltages has been performed in [11, 12] using both the Monte Carlo method and the transient simulation software EMTP. As outlined in [13], the conventional

Iranian Journal of Electrical & Electronic Engineering, 2026.
Paper first received 02 Aug 2025 and accepted 30 Jan 2026.
* The authors are with the Faculty of Electrical and Computer Engineering, University of Science and Technology of Mazandaran, Behshahr, Iran.
Corresponding Author: Nabiollah Ramezani.
E-mails: ramezani@mazust.ac.ir

Monte Carlo approach for assessing the lightning performance of distribution lines requires the generation of numerous incident scenarios. Each scenario is characterized by distinct lightning current waveform parameters and varying stroke locations. The lightning current parameters are derived from probability distributions obtained through lightning locating systems [14, 15]. Although the Monte Carlo method provides high-accuracy results, it suffers from two significant limitations. First, the network must be modeled separately for each point of interest. Second, a substantial number of simulations (typically on the order of 10,000 iterations per point) are required, resulting in considerable computational demands. Reference [16] evaluates the performance of low-voltage (LV) networks under lightning-induced overvoltages. However, this study neglects the influence of medium-voltage (MV) lines and their interconnection with LV networks through distribution transformers in the overvoltage computation. While [17, 18] present more comprehensive models of distribution networks, but these models do not account for spark-gap operation or its impact on overvoltage transfer through transformers. Reference [19] investigates the protection of low-voltage (LV) networks against lightning-induced overvoltages, including the effects of spark-gap operation. However, the study's reliance on Rusk's simplified formula, combined with an oversimplified grounding system model, compromises the reliability of its findings.

Despite extensive studies on lightning induced overvoltages in distribution networks, significant shortcomings are still observed in the existing methods and models. Monte Carlo-based methods and transient simulations, despite their high accuracy, face significant computational costs and require repeated network modeling for different points. On the other hand, many studies have either investigated low-voltage and medium-voltage networks separately or have not fully considered their interaction through distribution transformers. In addition, in some studies, the modeling of the nonlinear performance of the grounding system, together with spark gaps and overvoltage protection devices, in addition to the high-frequency behavior of network components, has not been considered, which can lead to inaccurate estimates of the level of transmitted overvoltages. Hence, there is a need for a comprehensive yet computationally efficient framework that can simultaneously cover accurate lightning modeling, the interaction of medium and low voltage networks, transformer behavior, grounding system, and the performance of protective equipment.

This paper investigates lightning-induced overvoltages in power distribution networks caused by nearby ground strikes through comprehensive Monte Carlo simulations. To reduce computational demands and simulation complexity, this study implements a constrained domain approach for overvoltage calculation. Using high-accuracy transient models, this study evaluates overvoltage propagation from indirect lightning strikes on the primary side of the transformer and subsequently, to the distribution network fed by this transformer. Furthermore, the study examines lightning strike effects on lightning protection systems (LPS) and evaluates the performance of protective devices, including spark gaps and surge protective devices (SPDs).

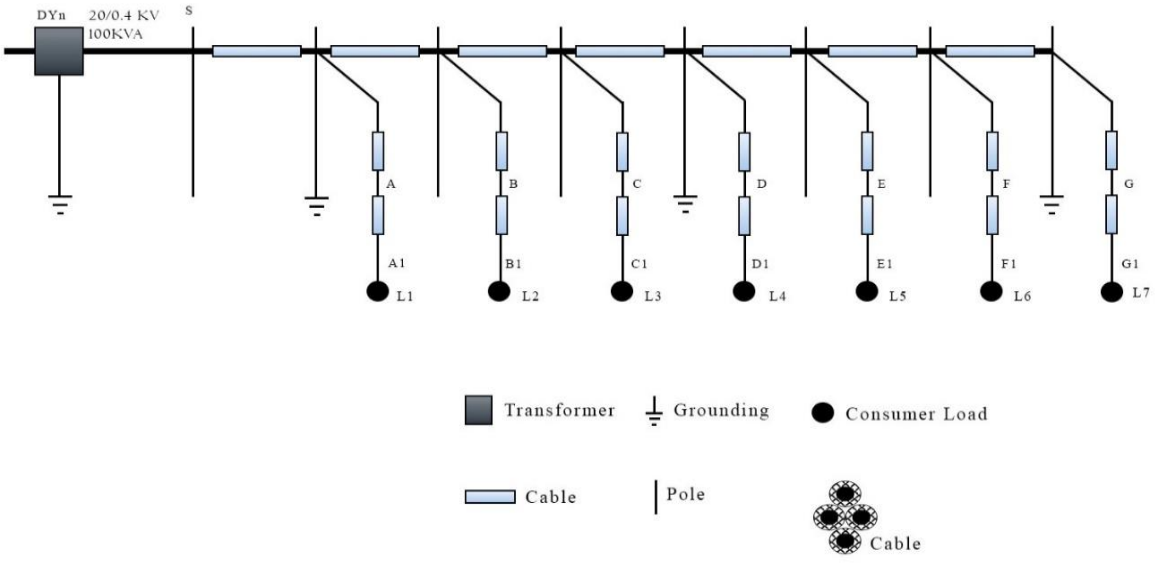

Fig 1. Single line diagram of the LV network

2 Transient Modeling of Distribution Network Components

2.1 Introduction of the Studied System

To investigate lightning-induced overvoltages, a simplified distribution test network (Fig. 1) was modeled in ATP-EMTP. The network comprises a low-voltage (LV) feeder consisting of seven overhead line sections, each with a length of 50 m, constructed from 4×35 mm² cable. The feeder supplies seven sensitive loads (L1 to L7). Each load is connected to the feeder via a service cable:

- Loads L1–L6 are connected using a 10 m long 4×10 mm² cable.
- Load L7 is connected using a 7 m long 5×10 mm² cable.

The LV system is configured as a three-phase TN-C network. The neutral conductor is grounded at the transformer location and at the end of each feeder section, as indicated in Fig. 1. All cable lengths and cross-sections are summarized in Table 1 below for clarity.

Table 1. Cable specifications in the test network [19]

Cable Type	Length (m)	Cross-section (mm²)	Purpose
Feeder section	50	4×35	Overhead line between nodes
Service cable (L1–L6)	10	4×10	Connection to loads L1–L6
Service cable (L7)	7	5×10	Connection to load L7

2.2 Indirect lightning strike

In this section, a set of indirect lightning strokes is produced using the Monte Carlo method. Subsequently, the lightning-induced overvoltage (LIOV) code is implemented in ATP-EMTP software to compute the resulting induced overvoltages. The obtained waveforms are generated through the following procedure:

In the initial step, numerous lightning events are stochastically generated. Each event is characterized by three key parameters: the front time (tf), peak current (Ip), and the perpendicular distance (y) between the lightning strike location and the line. The parameters tf and Ip define the lightning current waveform characteristics. Following established methodology [20], these parameters are modeled as log-normally distributed random variables.

With a correlation coefficient of 0.47 between these parameters, the negative first-stroke characteristics follow the probability distributions specified in Table 2.

Table 2. Log-normal distribution parameters for negative downward first strokes [20]

parameter	Madian parameter value		Standard deviation value of the parameter logarithm(base e)	
	(Ip≤20 KA)	(Ip>20 KA)	(Ip≤20 KA)	(Ip>20 KA)
Ip (KA)	61 KA	33.3KA	1.33	0.605
tf(μs)	3.83 μs		0.553	

In the subsequent step, a computational code (LIOV) is developed to calculate the peak induced voltage for each indirect lightning event. When the lightning strike occurs beyond a critical distance from the line or when the stroke current is below a threshold value, the resulting induced overvoltages become negligible for network protection considerations. Consequently, the analysis is confined to a defined region surrounding the line where lightning strokes may potentially affect the network.

In this study, each simulation run generates and analyzes 200 discrete points. Through 15 iterative simulations encompassing all operational states of the network under investigation, parameterized by peak current values and strike distances, we derive a bounded region characterizing the domain of lightning-induced overvoltage propagation.

As illustrated in Fig. 2, the points generated via the Monte Carlo method and located within the hatched region serve as inputs for the ATP-EMTP simulation study. Following the generation of 2000 lightning strokes using the Monte Carlo approach, the bounded region contains only 68 critical points, thereby significantly reducing both simulation time and computational burden.

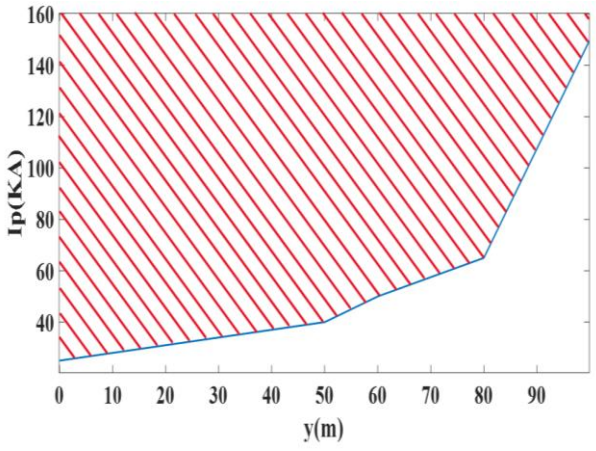

Fig 2. The area for chosen lightning strokes

Within the bounded region, eight representative waveforms (U1-U8) exhibiting distinct amplitudes, varying front times, and differing tail durations were

selected for analysis. These characteristic waveforms are presented in Fig. 3.

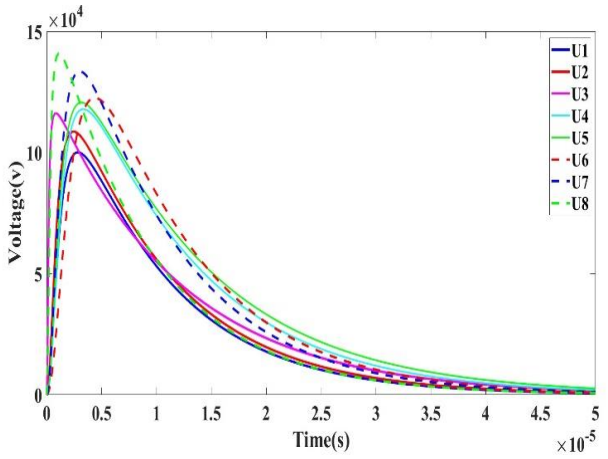

Fig 3. Waveforms generated by the Monte Carlo method

A critical issue involves the accurate modeling of the impulse current source injected into the LPS. The most straightforward implementation utilizes an internal ATP-EMTP library model consisting of a programmable current source with user-defined waveform characteristics. However, the input current waveform depends on both the generator parameters and the complete circuit characteristics, including the load impedance and grounding path that forms the current return loop to the generator [21]. Consequently, rather than employing an arbitrary current source, we adopt the actual impulse current generator model used in experimental testing and implement it in ATP-EMTP using its RLC parameters. This approach offers the additional advantage of enabling investigation of soil resistivity effects on the measured impulse current waveforms in the system [22]. Regard to prior research [22], the capacitor charging voltage is set to 34 kV. Figure 4 illustrates the lightning waveform generator model, while Table 3 provides its corresponding parameters.

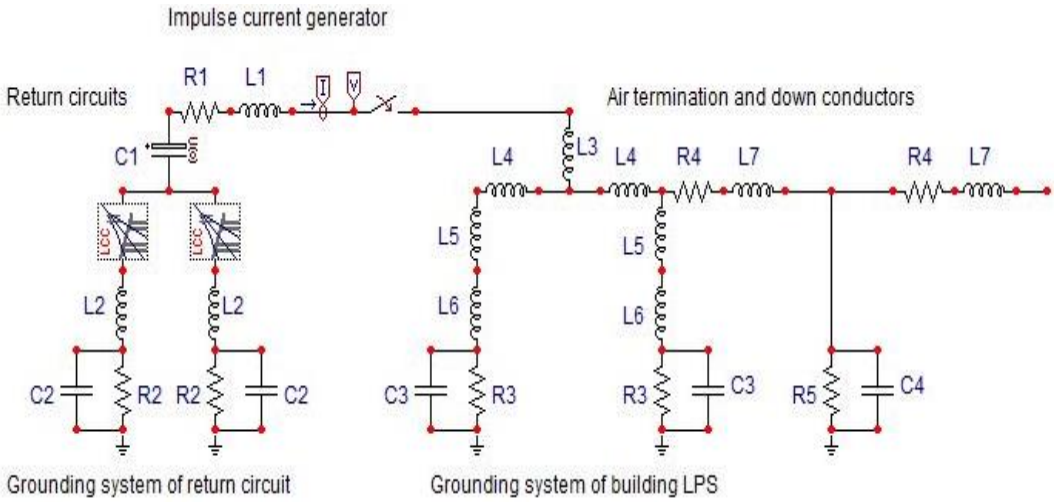

Fig 4. Lightning wave generator [22]

Table 3. Parameters of the lightning waveform generator [22].

R1 (Ω)	0.04	L4 (μH)	20
R2 (Ω)	8	L5 (μH)	29
R3 (Ω)	48.7	L6 (μH)	1.62
R4 (mΩ)	3.42	L7 (μH)	2.35
R5 (mΩ)	3.42	C1 (μF)	3.2
L1 (μH)	0.44	C2 (nF)	18
L2 (μH)	0.4	C3 (nF)	4.5
L3 (μH)	24	C4 (nF)	0.21

2.3 Model of the Transformer

To investigate the transferred overvoltages from the MV to LV network, a high-frequency distribution transformer model is essential. While numerous power transformer models exist in literature [23,24] and within the ATP-EMTP library, these are primarily suitable for network-frequency simulations. For high-frequency applications, we employ the distribution transformer model presented in [2,19] (Fig. 5), which specifically addresses the required frequency range.

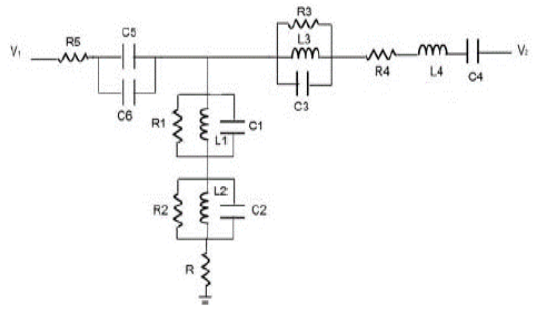

Fig 5. High-frequency model of distribution transformer [19]

The transformer model illustrated in Fig. 5 employs a two-port network representation using a T-equivalent circuit. Unlike conventional white-box models, which require intricate mathematical derivations and proprietary manufacturer data [25], the parameters of this model are derived experimentally through open-circuit tests conducted at two distinct resonance frequencies. The proposed transformer model operates effectively across a frequency range of 1 kHz to 10 MHz and is applicable under both no-load and loaded conditions. In addition to its simplicity, the model offers high accuracy, achieved by incorporating measurements at two distinct resonance frequencies during parameter extraction. Furthermore, time-controlled switches are employed to simulate the spark-gap behavior. Table 4 summarizes the derived parameters for a 100 kVA transformer protected by the spark-gap.

Table 4. Parameters of the high-frequency transformer model [19]

R1 (Ω)	500	L3 (mH)	0.036897
R2 (Ω)	558.5405	L4 (mH)	0.048296
R3 (Ω)	1000	C1 (µF)	0.021063
R4 (Ω)	10-6×1	C2 (µF)	0.00302967
R5 (Ω)	10-9×1	C3 (µF)	0.00512
R (Ω)	1500	C4 (µF)	0.00022167
L1 (mH)	0.00856	C5 (µF)	0.0004221
L2 (mH)	0.0046	C6 (µF)	0.00019152

2.4 The SPD Model

Nowadays, surge protective devices (SPDs) are extensively employed in distribution systems to safeguard sensitive equipment against lightning-induced overvoltages. These devices offer significant technical advantages, including:

- Highly nonlinear voltage-current characteristics,
- Minimal power losses under normal operating voltages,
- Exceptional operational reliability,
- Rapid response to transient overvoltages, and
- Long-term durability.

Accurate modeling of SPDs plays a critical role in insulation coordination studies, reliability assessments, and optimal SPD placement strategies. Consequently, significant research efforts have focused on developing precise SPD models to enhance system protection effectiveness. Class I SPDs are primarily designed to protect critical infrastructure equipped with lightning protection systems (LPS). For large-scale facilities (e.g., industrial plants or office complexes) requiring continuous operation - particularly those with backup power systems such as diesel generators or uninterruptible power supplies (UPS), etc. Class II SPDs with enhanced energy handling capacity (Type E or H) are recommended [26]. In installations without LPS, optimal protection can be achieved through:

- Installation of high-capacity Class II SPDs (Type H) at the service entrance for industrial facilities and large office complexes, or
- Deployment of Class II SPDs (Type E) for smaller-scale facilities.

In this paper, the Class I SPD of Type H, Class II SPD of Type E and Class II SPD of Type S have been utilized for the simulation experiments. To simulate the SPD in the ATP-EMTP environment, a variable resistor (MOV type) with a current-voltage diagram shown in Figs. 6 and 7 has been used.

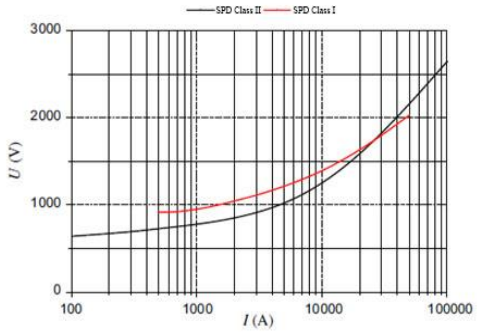

Fig 6. U/I diagram for Class I SPD of Type H and Class II SPD of Type E

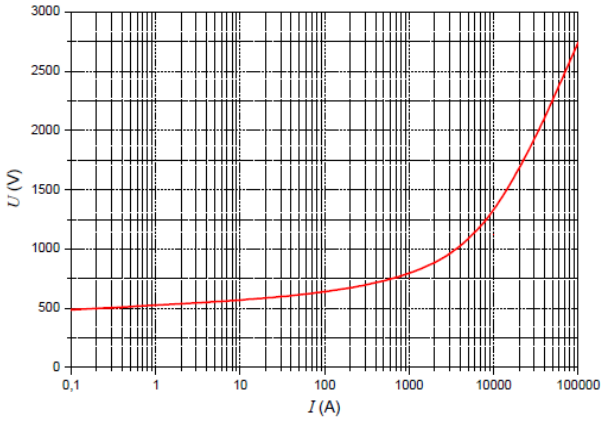

Fig 7. U/I diagram for Class II of Type S

2.5 The load Model

The overvoltage level in a distribution network is closely related to the connected loads. So, using accurate load models enhances the reliability of simulation results. In this study, we adopt the generalized load model proposed in [27]. Compared to other models in the literature, this model provides an accurate representation of high-frequency transient behavior in consumer loads. This model, compared to other models presented, is able to simulate the high-frequency transient behavior of the consumer well. In an experiment, ten residential buildings with different equipment were selected and their input impedance was measured over a wide frequency range from approximately direct current to 5 MHz, considering both amplitude and phase parameters. The equipment in the buildings included refrigerators, microwaves, dishwashers, washing machines, cordless phones, televisions, desktop computers, stereo systems, and DVD players. For each building, an equivalent circuit including resistors, inductors, and capacitors was modeled. Finally, these models were considered as a general model representing a group of residential installations for computational simulation. Fig. 8 illustrates the load model, while Table 5 summarizes its parameters. Additionally, Table 6 presents the basic insulation level (BIL) of the LV network equipment, as specified by the IEC 60664-1 standard.

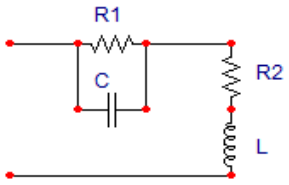

Fig 8. Model of the RLC load [27]

Table 5. Parameters of the RLC load [27]

R1(Ω)	R2(Ω)	L(μH)	C(nF)
100	2	5	100

Table 6. Insulation resistance of the LV netwrok equipment according to the IEC60644-1 Standard

Voltage class	Type of equipment	Max. Voltage (KV)
IV	equipment installed at the distribution board including measurement equipment, fuses and the main circuit	6
III	fuses and the main circuit	4
II	routine electrical equipment (home appliances)	2.5
I	sensitive electronic equipment like personal computers	1.5

2.6 Model of the Grounding System

A proper grounding system is essential to ensure the reliable performance of surge arresters, relays, and other protective devices. Moreover, such a system is needed to analyze lightning-induced overvoltages and their impact on network performance. To model the complex behavior of the grounding system under lightning strokes, resistors are commonly used to represent grounding systems [28]. Alternatively, a circuit-based approach offers a simplified method for high-frequency grounding system modeling, where parameters can be easily determined and implemented [29]. Among the available modeling methods, the transmission line approach offers a well-balanced representation of grounding systems. This method not only achieves good accuracy but also incorporates soil ionization effects in the system modeling. Due to its superior accuracy compared to circuit-theory-based and purely resistive models, the transmission line method (TLM) is employed in this study for grounding system modeling [30, 31]. The grounding system in different points of distribution network employs the following components:

- Transformer and SPDs: two cables (8 m and 11 m in length) along with 0.6 m galvanized steel rods (cross-section: 25 mm²).
- Network neutral: a 11 m cable and 0.6 m galvanized steel rods (cross-section: 25 mm²).
- Load: a 3 m galvanized steel rod.

The high-frequency model of the system is illustrated in Fig. 9.

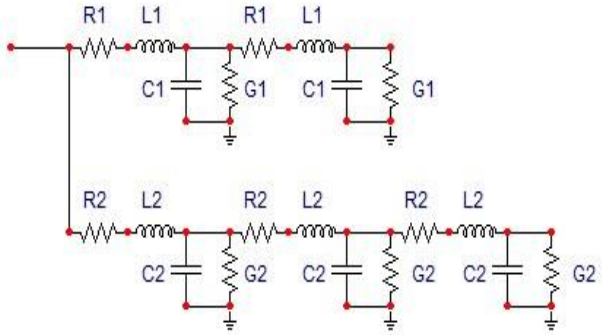

Fig 9. Model of grounding system

The grounding system parameters including equivalent resistance, capacitance, inductance, and conductance are calculated using Eqs. (1)–(6). To calculate these parameters, the values of conductivity and relative permittivity of the electrode are considered equal to $\sigma = 0.002\ s/m$ and $\varepsilon_r = 10$, respectively.

$$R = \frac{\rho_0 \times l}{2 \times \pi \times a \times \delta} \tag{1}$$

$$L = \frac{\mu_0 \times l}{2 \times \pi}\left[\ln \frac{2l}{\sqrt{2 \times h \times a}} - 1\right] \tag{2}$$

$$C = \frac{2 \times \pi \times \varepsilon \times l}{\left[\ln \frac{2 \times l}{\sqrt{2 \times h \times a}} - 1 \right]} \quad (3)$$

$$R(t) = \frac{R_0}{\sqrt{1 + \frac{I}{I_g}}} \quad (4)$$

$$G(t) = \frac{2 \times \pi \times l}{\rho_s \times \left[\ln \frac{2 \times l}{\sqrt{2 \times h \times a}} - 1 \right]} \times \sqrt{1 + \frac{I(t)}{I_g}} \quad (5)$$

$$I_g = \frac{E_{cr} \times \rho_s}{2 \times \pi \times R_0^{\,2}} \quad (6)$$

The calculated parameters are shown in Table 7.

Table 7. Parameters of the Grounding System

R1(mΩ)	6.84	L1(μH)	4.70
G1(Ω)	39.8	L2(μH)	4.24
R2(mΩ)	6.16	C1(nF)	0.21
G2(Ω)	44.2	C2(nF)	0.19

In Table 7, l, a, and h respectively stand for the length, radius, and depth of the electrode burial, all in meters. ρ_s is the soil resistivity (100 Ω/m), ε_r is the relative dielectric constant of the soil, ε_0 is the vacuum dielectric constant (8.8419×10-12 F/m), and μ0 is the vacuum permeability (1.256×10-6 H/m). Also, δ is the skin effect coefficient, ρ_s is the specific resistivity of the conductor, R0 is the static resistivity of the soil (Ω), and R(t) and G(t) are, respectively, the nonlinear resistivity (Ω) and the conductivity (υ) of the ground electrode. Moreover, I(t) is the electrode current caused by the lightning and Ig is the current limit from which the soil ionization occurs (both in amperes).

2.7 Model of the line and cable

The XLPE cable is simulated using the line and cable constants (LCC) model in ATP-EMTP software, which implements the JMarti frequency-dependent line model. This approach accurately represents the cable's admittance characteristics and diffusion properties through rigorous mathematical formulations. While computationally more demanding than alternative models available in the software library, the JMarti-based LCC model delivers enhanced simulation accuracy [19]. Fig. 10 presents the computational framework for analyzing lightning-induced overvoltages in the system.

The dimensions and parameters of the cable used in the simulation are as follows:

• Conductor cross-section= 35 mm^2 ;

• Outer insulation thickness= 1.6 mm;

• Conductor resistivity= 2.84×10^{-9} Ω.m;

• Relative permeability of the conductor material= 1 ;

• Relative permeability of the insulator material outside the Conductor= 1;

• Relative permittivity of the insulator material outside the conductor= 2.3.

3 Simulation Scenarios

In order to analyze lightning-induced overvoltages transferred to the low-voltage (LV) network and to evaluate the performance of protective devices, several simulation scenarios were investigated within a limited study area using the Monte Carlo method. In all scenarios, high-frequency models of distribution network components and the distribution transformer were considered.

3.1 Simulation of the Low-Voltage Network without Spark-Gap and SPD

In this scenario, the LV test network was simulated without Spark-Gap and surge protective devices (SPDs) to determine the level of overvoltages transferred from the upstream network and the distribution transformer to the LV side. This scenario was considered as the reference case for comparison with other protective configurations, and the voltage stress imposed on sensitive loads was evaluated.

3.2 Simulation of the Network with Spark-Gap Modeling on the Transformer Primary Side

In this scenario, a Spark-Gap was modeled on the primary side of the distribution transformer. The operation of the Spark-Gap leads to a sudden truncation of the lightning current waveform and a rapid change in the current rate of rise (di/dt). This phenomenon results in increased induced voltages and transient overvoltages in the low-voltage network. Although the Spark-Gap effectively discharges the lightning current and provides protection for the transformer, the abrupt current interruption may cause higher voltage peaks and more severe overvoltage transfer to the LV network. The impact of this effect on the LV voltage levels and connected loads was analyzed in this scenario.

3.3 Installation of Class I SPD at the Beginning of the Low-Voltage Feeder

In this scenario, a Class I SPD was installed at the incoming feeder of the LV network. The objective was to assess the capability of the Class I SPD to discharge high-magnitude lightning currents and reduce the amplitude of overvoltages transferred from the transformer to the LV network. The residual voltage after SPD operation was evaluated.

3.4 Application of Class II SPD in the Internal Low-Voltage Network

Subsequently, a Class II SPD was simulated in the internal distribution boards of the LV network. This scenario aimed to investigate supplementary protection

of the LV network and sensitive electronic loads against lower-magnitude and residual overvoltages remaining after the operation of the Class I SPD. Coordination between Class I and Class II SPDs was also analyzed.

3.5 Direct Lightning Strike to the Load LPS and Its Impact on the Low-Voltage Network

In this scenario, a direct lightning strike to the load lightning protection system (LPS) was simulated, and its effects on the LV network and sensitive loads were investigated.

3.6 Installation of SPD Near the Load for Direct Load Protection

In the final scenario, an SPD was installed close to sensitive loads to analyze the remaining overvoltage at the load terminals. This scenario demonstrates the role of SPDs in reducing insulation stress on electronic equipment and improving the overall protection level of the low-voltage network.

4 Simulation Results and Discussion

The network under study is depicted in Fig. 1. The simulation employs overvoltages generated via the Monte Carlo method, which serve as the lightning excitation source on the primary side of the distribution transformer (Fig. 3). This impulse waveform represents an indirectly induced overvoltage characterized by a significantly shorter tail time compared to that of the lightning current waveform. The induced overvoltages are evaluated under the following scenarios:

- Lightning strikes to nearby MV lines;
- Protective effects of spark gaps on the transformer
- Impact of SPD installation on the transformer secondary side for LV network protection
- Lightning strikes to the LPS and associated overvoltage propagation through the LV network
- Effectiveness of SPDs in overvoltage mitigation and load protection

4.1 The computation of overvoltages transferred through the transformer without considering the spark-gap

This study investigates the characteristics of overvoltages transferred from the HV to LV side of a power transformer when spark-gap protection is not implemented. The research focuses on a radial distribution network configuration, with comprehensive waveform measurements taken at three strategic locations (S, A1, and G1 in Fig. 11).

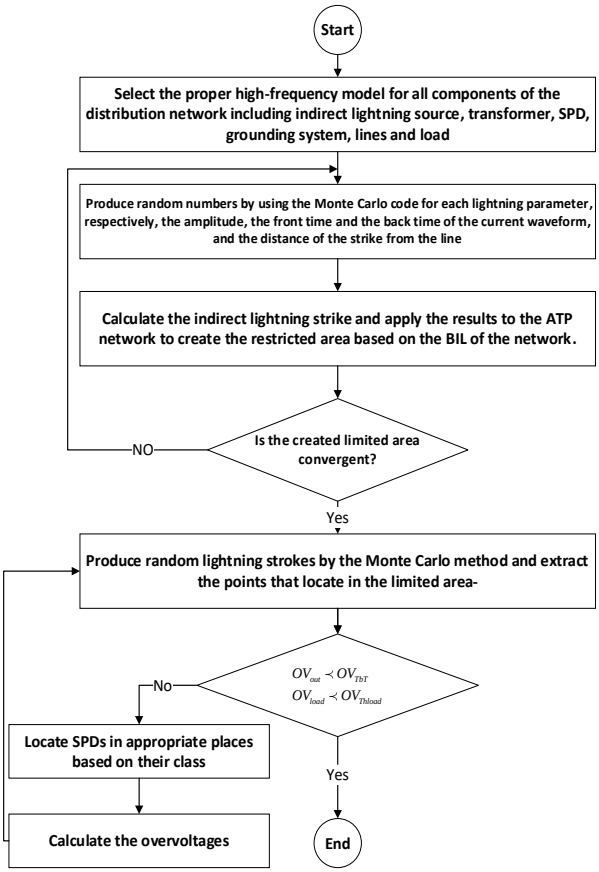

Fig 10. The proposed flowchart to compute the lightning overvoltages

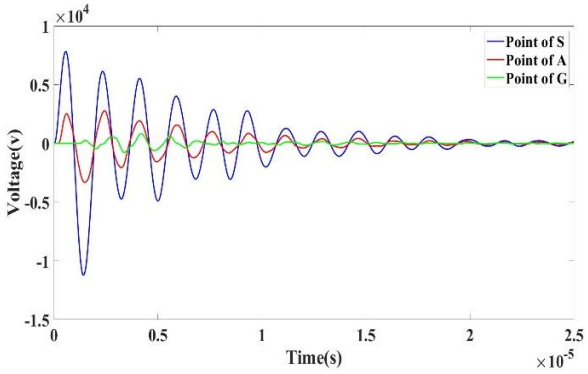

Fig 11. Transferred overvoltages through the transformer for the waveform U1 in the absence of the spark-gap

The maximum values of the overvoltage at points S, A1, and G1 are given in Table 8.

Table 8. Transferred overvoltages through the transformer without using the spark-gap protection - lightning waveform- Location of the measurement

Overvoltage measurement locations (V)								Lightning waveform
G	F	E	D	C	B	A	S	
820	**2165**	**2200**	**1190**	**3370**	**4000**	**2781**	**7830**	U1
1320	**3450**	**3580**	**1940**	**5400**	**6480**	**4160**	**11250**	U2
6785	**13410**	**16100**	**8450**	**24550**	**20550**	**23670**	**43660**	U3
710	**1860**	**1870**	**1020**	**2880**	**3380**	**2440**	**7420**	U4
890	**2360**	**2390**	**1290**	**3660**	**4330**	**3040**	**8740**	U5
275	**724**	**705**	**386**	**1050**	**1167**	**1270**	**4050**	U6
945	**2510**	**2510**	**2530**	**1370**	**3885**	**4585**	**9480**	U7
5175	**13100**	**14570**	**7760**	**22420**	**21740**	**18560**	**40150**	U8

The experimental results presented in Table 8 demonstrate a strong correlation between lightning waveform characteristics and resultant overvoltage magnitudes. Specifically, the measured overvoltage levels generated by waveforms U2, U3, and U8. The shorter the front duration, the higher the resulting overvoltages. Additionally, as the distance from the feeder's origin increases, the overvoltages gradually decrease and are attenuated along the line. This attenuation is more pronounced in lines A, D, and G, where the network neutral is grounded.

4.2 The computation of overvoltages transferred through the transformer considering the spark-gap

In this section, the simulation is performed using a spark-gap, and the transferred overvoltages are measured at points S, A, B, C, D, E, F, and G. The maximum values of the overvoltages at these points are presented in Table 9. Fig. 12 illustrates the overvoltages transferred through the transformer protected by the spark-gap at points S, A, and G.

Table 9. Transferred overvoltages through the transformer with the the spark-gap protection- lightning waveform- Location of the measurement

Overvoltage measurement locations (V)								Lightning waveform
G	F	E	D	C	B	A	S	
11850	**19000**	**14350**	**12160**	**23100**	**21400**	**26500**	**45700**	U1
12450	**21450**	**15400**	**21500**	**23700**	**22600**	**27000**	**45000**	U2
13050	**16750**	**16100**	**13150**	**27250**	**28300**	**36850**	**71250**	U3
14400	**24300**	**17380**	**15080**	**28540**	**26400**	**32600**	**57500**	U4
14670	**24660**	**17700**	**15150**	**28750**	**26750**	**32940**	**58000**	U5
15060	**23500**	**18200**	**16270**	**30000**	**27500**	**31000**	**58400**	U6
15990	**26850**	**19300**	**16600**	**31300**	**29050**	**36100**	**63000**	U7
14770	**19260**	**18230**	**18240**	**32750**	**33650**	**44700**	**86050**	U8

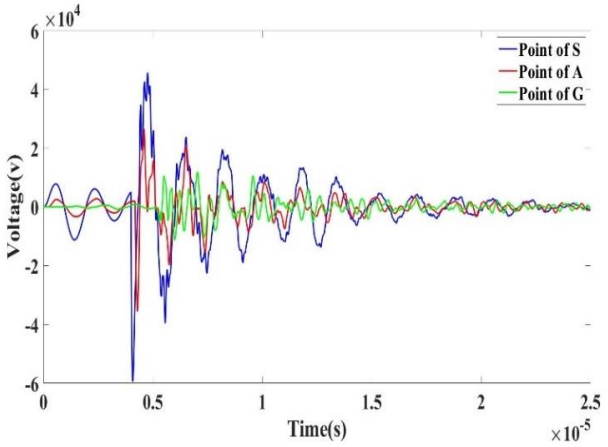

Fig 12. Transferred overvoltages through the transformer for the waveform U1 in the presence of spark-gap

The simulation results indicate that during spark-gap operation, the overvoltages transferred to the LV network increase. This is attributed to the dynamic interaction between the impulse generator and the transformer through the spark-gap discharge. This finding has also been verified in [2] through practical tests and simulation results using ATP-EMTP. According to Table 9, due to the low Basic Insulation Level (BIL) of the LV network and the presence of sensitive electronic loads, the transferred overvoltages can potentially damage both the loads and the LV network.

4.3 The computation of overvoltages transferred through the transformer in the presence of SPD

Since the use of a spark-gap increases overvoltages and may lead to damage in the network, Surge Protective

Devices (SPDs) are employed to mitigate this issue and protect the LV network. The installation method for the SPDs is described in the following section.

- **The computation of overvoltages transferred through the transformer in the presence of Class I SPD**

To protect the network against overvoltages caused by spark-gap operation on the primary side of the transformer, a Class I SPD is installed at the beginning of the feeder. Subsequently, the resulting overvoltages are measured and compared. Lightning waveforms are applied to the MV side of the transformer, and the overvoltages transferred through the transformer are measured at points S, A, B, C, D, E, F, and G. The results of the lightning strike in the presence of the SPD are presented in Fig. 13. The maximum overvoltage values at points S, A1, and G1 are listed in Table 10.

According to Fig. 13(a), the installation of a Class I SPD results in a reduction of overvoltages by approximately 500 V (equivalent to 0.3333 per unit of the LV network BIL) prior to spark-gap operation. However, after the spark-gap operation, the overvoltages initially increase to 680 V (0.4544 per unit of the LV network BIL) and are then damped to zero within approximately 50 μs. As the distance from point S increases, despite the occurrence of overvoltage resonance, the transient overvoltages rise and subsequently decrease to approximately 525 V at the end of the line (see Fig. 13(b)).

- **The computation of overvoltages transferred through the transformer with the joint use of Class I and Class II SPDs**

Due to the resonance phenomenon, the transferred overvoltages increase along the feeder, posing a risk to sensitive electronic loads and computers. To mitigate resonance, reduce overvoltages, and protect sensitive equipment, a Class II SPD is installed at a distance of 7 meters from the first SPD. The resulting overvoltages after the installation of this additional SPD are presented in Table 11.

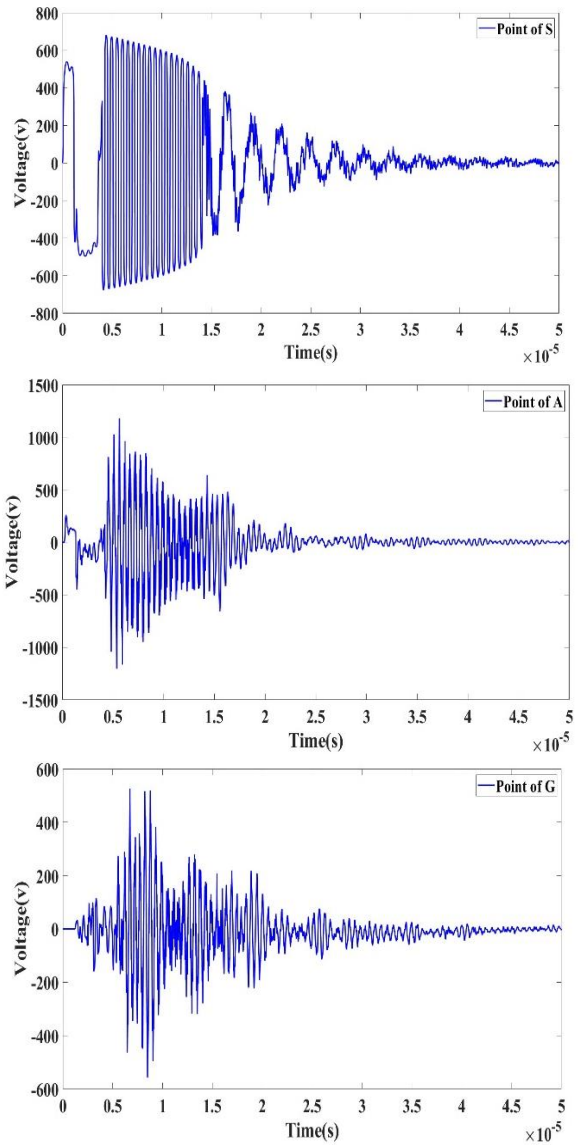

Fig 13. Transferred overvoltages through the feeder protected by a Class I SPD- (a) the overvoltage measured at point S - (b) the overvoltage measured at point A- (c) the overvoltage measured at point G

Table 10. Transferred overvoltages through the transformer in the presence of a class I SPD

Overvoltage measurement locations (V)								Lightning waveform
G	F	E	D	C	B	A	S	
525	420	380	425	700	1600	1180	681	U1
520	430	460	425	740	1565	1190	684	U2
770	485	435	530	1090	2000	2050	684	U3
500	405	338	368	745	1640	1215	693	U4
538	385	330	415	725	1600	1200	694	U5
528	430	400	375	735	1560	1220	695	U6
525	410	334	387	750	1640	1230	700	U7
730	552	578	715	1225	2105	2115	689	U8

Table 11. Transferred overvoltages from the transformer to the feeder protected by the Class I and Class II SPDs

Overvoltage measurement locations (V)								Lightning waveform
G	F	E	D	C	B	A	S	
7	8	6	7	7	16	26	672	U1
6	4	5	6	10	14	25	685	U2
6	4	4	6	9	15	35	685	U3
7	6	6	6	9	12	23	694	U4
6	4	5	7	10	14	25	695	U5
7	6	7	8	10	19	34	696	U6
6	5	6	6	9	11	31	700	U7
6	4	5	6	10	14	26	690	U8

According to Table 11, at point S, the level of transient overvoltages decreases to approximately 680 V (0.4533 per unit of the LV network BIL) after the installation of the Class I SPD. Furthermore, following the installation of the Class II SPD, most of the remaining energy is discharged by the first SPD, resulting in a further reduction of the overvoltage to approximately 20 V. Finally, these overvoltages are completely damped within about 20 μs. As observed in Table 11, when the Class II SPD is installed within an appropriate distance from the Class I SPD, the overvoltage levels along the feeder decrease to below 30 V (0.02 per unit of the LV network BIL), which is considered acceptable for sensitive electronic equipment. Another aspect investigated in this study is the effect of varying distances between the Class I and Class II SPDs. Initially, the Class II SPD is installed after the first line (at a distance of 50 meters), and the overvoltages transferred through the transformer are measured at points S to G. Subsequently, the Class II SPD is relocated to the next line (at a distance of 100 meters), and the overvoltages are measured again. This procedure is repeated for all lines, and the maximum values of the transferred overvoltages corresponding to each location of the second SPD are presented in Table 12. Based on the overvoltages presented in Table 12, it can be concluded that placing the SPD at an inappropriate distance has a negligible effect on overvoltage reduction in the network, with significant voltage reduction occurring only at the SPD installation point.

Table 12. Transferred overvoltages from the transformer by changing the location of Class II SPD

Overvoltage measurement locations (V)								Placement distance of SPD class I
G	F	E	D	C	B	A	S	
10	10	15	18	28	50	58	690	50 m
447	685	905	558	666	54	3522	690	100 m
725	715	870	100	46	1375	1173	690	150 m
490	295	450	33	700	1185	1970	690	200 m
615	390	47	730	700	1160	1625	690	250 m
810	50	560	572	476	1360	1570	690	300 m
85	440	505	525	995	1430	1650	690	350 m

4.4 The effect of lightning strike on the LPS and the investigation of its induced overvoltages along the feeder

First, a lightning waveform is applied to the LPS load L7. Of the overvoltages induced by the indirect lightning strike, some dissipate into the ground through the building's grounding system, some are transferred to the load, and the remainder are distributed along the feeder. The maximum values of lightning-induced overvoltages at points G1 to S are presented in Table 13. Additionally, example waveforms at points G1, F1, and A1 are illustrated in Fig. 14.

Table 13. Transferred overvoltages through the transformer in the absence of SPD

Measured overvoltages (V)	Overvoltage measurement locations
6	S
542	A1
1807	B1
1620	C1
1200	D1
4119	E1
4330	F1
7067	G1

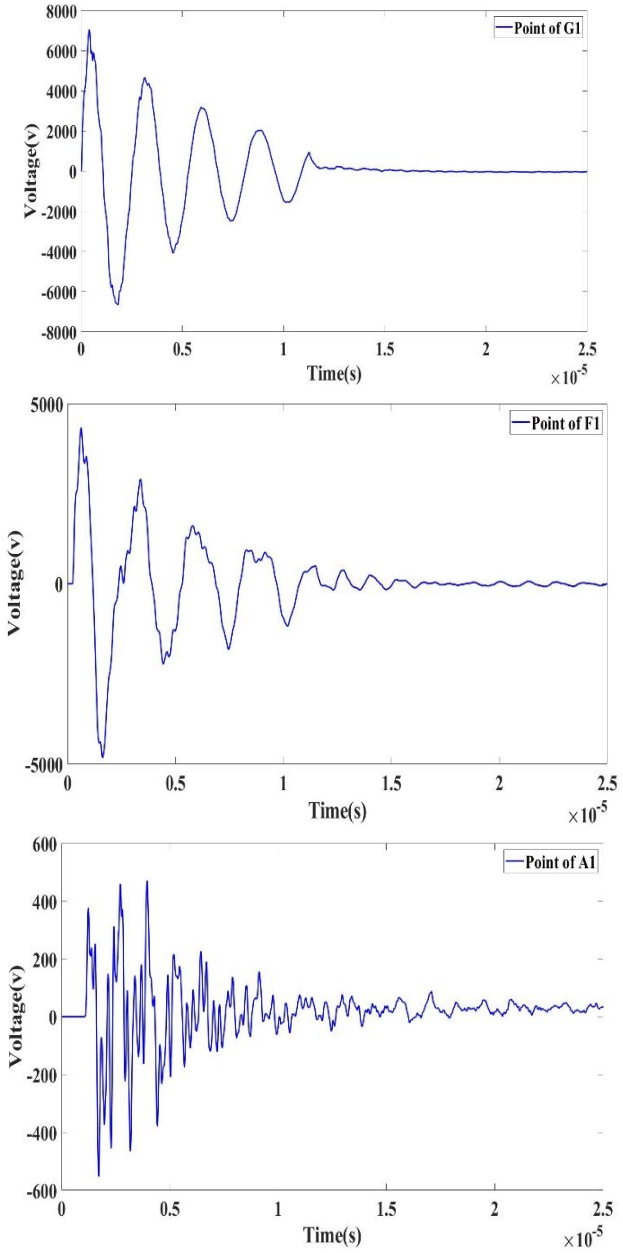

Fig 14. Transferred overvoltages induced by indirect lightning strike on the LPS - (a) the overvoltages measured at point G1 - (b) the overvoltages measured at point F1- (c) the overvoltages measured at point A1

As shown in Fig. 14(a), the lightning strike on the LPS induces a transient overvoltage with a peak value of 7 kV. Additionally, overvoltages are transferred to other loads (Fig. 14(b)) and are completely damped after approximately 12 μs.

As shown in Table 13, a direct lightning strike on the LPS of load L7 results in a 7 kV overvoltage (4.6 per unit of the LV network BIL) at point G1. This overvoltage propagates throughout the network, affecting other loads as well. As the distance from the lightning strike location increases, the induced overvoltages decrease, particularly beyond sections where the neutral is grounded. Nevertheless, the overvoltage levels remain excessive and pose a risk of damage to the loads. To mitigate these overvoltages and protect the equipment, a Class II SPD (Type S) is employed.

4.5 The effect of lightning strike on the LPS of the SPD-protected load and studying its overvoltages transferred through the feeder

A Class II SPD of Type S is installed at point G1 on load L7. Subsequently, the simulation is performed considering a lightning strike on the LPS of load L7. The peak values of the induced overvoltages are presented in Table 14, and the corresponding waveforms are shown in Fig. 15.

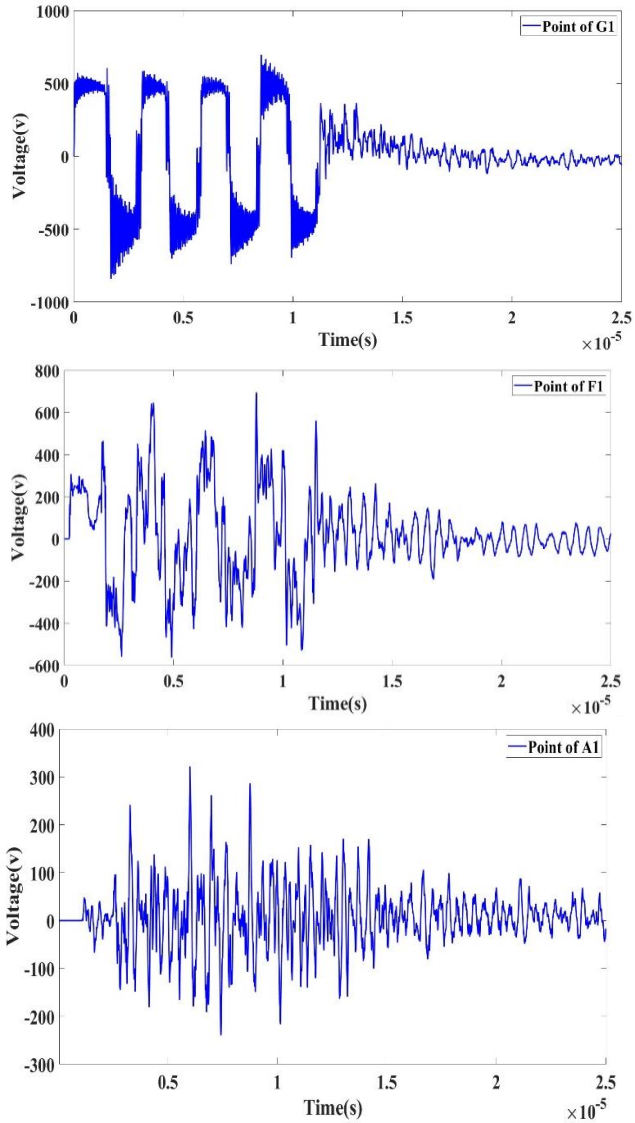

Fig 15. Transferred overvoltages transferred to the load protected by a Class II SPD - (a) the overvoltages measured at point G1 - (b) the overvoltages measured at point F1- (c) the overvoltages measured at point A1

As shown in Fig. 15(a), the additional SPD limits the lightning-induced overvoltages to approximately 690 V (0.46 per unit of the LV network BIL) at the point of the lightning strike. However, in this scenario, the reduction and damping of overvoltages occur over a longer duration of about 25 μs. The transient overvoltages transferred to adjacent loads are similarly reduced and fully damped after 25 μs, as illustrated in Figs. 15(b) and 15(c).

Table 14. Transferred overvoltages to the load protected by a class II SPD

Measured overvoltages (V)	Overvoltage measurement locations
260	S
320	A1
450	B1
485	C1
409	D1
690	E1
685	F1
690	G1

The simulation results indicate that adding a Class II SPD reduces the overvoltage at the lightning strike point to approximately 700 V (0.4666 per unit of the LV network BIL), with complete damping occurring after 25 μs. Additionally, the overvoltages transferred to other lines are reduced, and their magnitude decreases further with increasing distance from the strike point.

5 Conclusion

This paper investigates the effects of lightning-induced overvoltages on distribution networks using high-frequency accurate models of network components and by considering key parameters influencing the overvoltages. Based on the results of this study, appropriate protective solutions are proposed to mitigate the effects of these overvoltages. Due to the complex computations involved in analyzing overvoltages caused by indirect lightning strikes, this topic has received limited attention in the literature. This paper employs the Monte Carlo method to define a limited area for calculating the generated lightning waveforms, significantly reducing simulation time and computational burden.

The results indicate that shorter lightning wavefront durations correspond to higher amplitudes of overvoltages induced in the network. Additionally, spark-gap operation increases the overvoltages transferred through the transformer. Therefore, if a network is protected using a spark-gap, its operation must be taken into account during the design of the network insulation.

By appropriately installing SPDs, the overvoltages transferred through the transformer can be reduced to acceptable levels. However, improper installation of SPDs has little effect on overvoltage reduction. By installing a Class I SPD, the overvoltages transferred from the transformer to the LV feeder are reduced from 45,700 V to 1,600 V (1.06 per unit of the LV network BIL). Subsequently, the addition of a second SPD (Class II) further decreases the overvoltages to 26 V.

Conflict of Interest Statement

The authors declare that they have no conflicts of interest.

Funding

No funding was received for this work

References

[1] M. S. Vieira, and J. M. Janiszewski, "Propagation of lightning electromagnetic fields in the presence of buildings," *Electric power systems research*, vol. 118, pp. 101-109, 2015.

[2] N. A. Sabiha, I. A. Hend, and L. Matti, "High frequency modeling and experimental verification of distribution transformers using transfer function approach," *Electric Power Systems Research*, vol. 204, pp. 107671, 2022.

[3] F. H. Silveira, and S. Visacro, "Evaluation of lightning-induced voltages on low-voltage distribution networks," *IX International Symposium on Lightning Protection*, pp. 335-340, 2007.

[4] J. Cao, Y. Du, Y. Ding, R. Qi, B. Li, M. Chen, and Z. Li, "Practical schemes on lightning energy suppression in arresters for transformers on 10 kV overhead distribution lines," *IEEE Transactions on Power*, vol. 113, pp. 121-128, 2014.

[5] F. O. Resende and J. A. Peças Lopes, "Using low-voltage surge protection devices for lightning protection of 15/0.4 kV pole-mounted distribution transformer," *CIRED Open Access Proc. J.*, vol. 2017, no. 1, pp. 888–892, 2017.

[6] De Conti, F. H. Silveira, and S. Visacro, "On the role of transformer grounding and surge arresters on protecting loads from lightninginduced voltages in complex distribution networks," *Electric Power Systems Research*, vol. 113, pp. 204-212, 2014.

[7] De Conti, F. H. Silveira, and S. Visacro, "On the role of transformer grounding and low-voltage surge arresters on protecting loads in complex distribution networks," *2012 International Conference on Lightning Protection (ICLP). IEEE*, pp. 1-7, 2012.

[8] J. O. S. Paulino, C. F. Barbosa, I. J. S. Lopes, and W. C. Boaventura, "Assessment and analysis of indirect lightning performance of overhead lines," *Electr. Power Syst. Res.*, vol. 118, pp. 55–61, Jan. 2015.

[9] F. Mahmood, N. A. Sabiha, and M. Lehtonen, "Probabilistic Risk Assessment of MV Insulator Flashover under Combined AC and Lightning-Induced Overvoltages," *IEEE Trans. Power Deliv.*, vol. 30, no. 4, pp. 1880–1888, 2015.

[10] Andreotti, F. Mottola, M. Pagano, L. Verolino, "Lightning induced voltages on power lines: a new statistical approach", *Electrical Drives Power Electronics*, pp. 445-451, July. 2008.

[11] M. Dudurych, T. J. Gallagher, M. Holly, "A novel stochastic approach to the assessment of the lightning performance of HV transmission lines using EMTP", *IEEE Power Tech Conference Proceedings*, vol. 1, 8 pp, June. 2004.

[12] A. Martinez, F. Castro-Aranda, "Lightning performance analysis of overhead transmission lines using the EMTP", *IEEE Trans on Power Delivery*, vol. 20, pp. 2200-2210, June. 2005.

[13] Borghetti, C. A. Nucci, and M. Paolone, "An Improved Procedure for the Assessment of Overhead Line Indirect Lightning Performance and Its Comparison with the IEEE Std. 1410 Method," *IEEE Trans. Power Deliv.*, vol. 22, no. 1, pp. 684–692, 2007.

[14] CIGRE WG C4.407, "Lightning parameters for engineering applications," CIGRE Technical Brochure 549, Paris, France, 2013.

[15] CIGRE WG C4.404, "Cloud-to-ground lightning parameters derived from lightning location systems: The effects of system performance," CIGRE Technical Brochure 376, Paris, France, 2009.

[16] F. H. Silveira, and S. Visacro, "Evaluation of lightning-induced voltages on low-voltage distribution networks," *IX International Symposium on Lightning Protection*, pp. 335-340, 2007.

[17] A. De Conti, F. H. Silveira, and S. Visacro, "On the role of transformer grounding and low-voltage surge arresters on protecting loads in complex distribution networks," *2012 International Conference on Lightning Protection (ICLP). IEEE*, pp. 1-7, 2012.

[18] A. De Conti, F. H. Silveira, and S. Visacro, "On the role of transformer grounding and surge arresters on protecting loads from lightninginduced voltages in complex distribution networks," *Electric Power Systems Research*, vol. 113, pp. 204-212, 2014.

[19] N. A. Sabiha and M. Lehtonen, "Lightning-induced overvoltages transmitted over distribution transformer with MV spark-gap operation—Part II: Mitigation using LV surge arrester," *IEEE Transactions on Power Delivery*, vol. 25, no. 4, pp. 2565–2573, 2010.

[20] A. Borghetti, C. A. Nucci, and M. Paolone, ''An improved procedure for the assessment of overhead line indirect lightning performance and its comparison with the IEEE Std. 1410 method,'' *IEEE Trans. Power Del*., vol. 22, no. 1, pp. 684–692, Jan. 2007.

[21] B. Wang, Z.-C. Fu, and N.-N. Yan, "Design of multi-component impulse current generator for practical lightning current simulation," in *Proc. Int. Conf. Lightning Protection, Shanghai*, pp. 278–282, China, 2014

[22] G. Maslowski and S. Wyderka, "Modeling of currents and voltages in the lightning protection system of a residential building and an attached overhead power line," *IEEE Trans Electromagn Compat*, vol. 62, no. 5, pp. 2164–2173, 2020.

[23] E. Rahimpour and M. Bigdeli, ''Simplified transient model of transformer based on geometrical dimensions used in power network analysis and fault detection studies,'' *in Proc. Int. Conf. Power Eng., Energy Electr. Drives*, pp. 375–380, 2009.

[24] B. Jurisic, A. Xemard, I. Uglesic, F. Paladian and P. Guuinic, "Case Study on Transformer Models for Calculation of High Frequency Transmitted Overvoltages", *CIGRE 3rd International Colloquium "Transformer Research and Asset Management"*, Split, 2014.

[25] E. E. Mombello and G. A. Diaz Florez, "An improved high frequency white-box lossy transformer model for the calculation of power systems electromagnetic transients," *Electric Power Systems Research*, vol. 190, p. 106838, 2021.

[26] Piparo, GB Lo, R. Pomponi, T. Kisielewicz, C. Mazzetti, and A. Rousseau. "Protection against lightning overvoltages: Approach and tool for surge protective devices selection." *Electric Power Systems Research* 188, pp. 106531, 2020.

[27] Bassi, Welson. "High frequency input impedance modeling of low-voltage residential installations-influence on lightning overvoltage simulations results." *SpringerPlus* 3, no. 1, pp. 1-11, 2014.

[28] S. Pili˘ski´c, I. Ugle˘si´c, B. Juri˘si´c, "Evaluating the overvoltage performance of an overhead line taking into account the frequency-dependence of its tower's grounding electrodes with high soil resistivity," *International Journal of Electrical Power & Energy Systems*., vol. 116, p.105547, 2020.

[29] P. Yutthagowith, ''A modified pi-shaped circuit-based model of grounding electrodes,'' *2016 33rd International Conference on Lightning Protection (ICLP). IEEE*, pp. 1–4, 2016.

[30] G. Maslowski, S. Wyderka, R. Ziemba, G. Karnas, K. Filik, And L. Karpinski, "Measurements and modeling of current impulses in the lightning protection system and internal electrical installation equipped with household appliances*," Electric Power Systems Research, vol. 139*," pp. 87-92, 20, 2015.

[31] D.S. Gazzana, A.S. Bretas, G.A.D. Dias, M. Telló, D.W.P. Thomas, C. Christopoulos, "The transmission line modeling method to represent the soil ionization phenomenon in grounding systems," *IEEE Trans. Magn. 50*, no. 2, pp. 505-508, 2014.

Biographies

Peyman Gholami was born in Guilan, Iran. He received the B.Sc. degree in Electrical engineering from the Islamic Azad University, Lahijan branch, Iran, in 2022 and the M.Sc. degree in Electrical engineering from University of Science and Technology of Mazandaran, Behshahr, Iran, in 2025. His research interests include modeling of power systems and transient study in power system.

Nabiollah Ramezani was born in Babol, Iran, in 1972. He received the B.Sc. in Electrical Engineering from K.N.T. University of Science and Technology, in 1996 and M.Sc. and the Ph.D. degrees both in Electrical Engineering from Iran University of Science and Technology (IUST), Tehran, Iran, in 1999 and 2008 respectively. He is currently an Associate

Professor in the Department of Electrical and Computer Engineering, University of Science and Technology of Mazandaran, Behshahr, Iran. He is also the head of the power system protection and relay laboratory. His research interest includes protection and transient study in power systems.

Faridoddin Safaei was born in Mazandaran Iran, in 1990. He received the B.Sc. degree in Electrical engineering from the Shahid Abbaspour University, Tehran, Iran, in 2013 and the M.Sc. degree in Electrical engineering from University of Science and Technology of Mazandaran, Behshahr, Iran, in 2015. Also, He received the Ph.D. degree in Semnan University, Iran, in 2023. His research interests include power systems analsis and transient study in power systems.